ISSN 2348-1218 (print)
International Journal of Interdisciplinary Research and Innovations ISSN 2348-1226 (online)
Vol. 12, Issue 2, pp: (55-66), Month: April 2024 - June 2024, Available at: www.researchpublish.com

Magnetic Induction Effects on Unsteady Viscous Casson Fluid Flow over a Stretching Sheet

Christine Muthui[1], Charles Muli[2], Mark Kimathi[3]

[1,2,3] Mathematics and Statistics Department.

[1,2,3] Machakos University, Machakos, Kenya.

DOI: https://doi.org/10.5281/zenodo.12543989

Published Date: 26-June-2024

Abstract: **This study examines the impact of an induced magnetic field on the behaviour of an unsteady viscous Casson magneto hydrodynamic (MHD) fluid flow over a stretching sheet. The Casson fluid flow is influenced by a uniform external magnetic field that is applied perpendicular to the stretching sheet. The problem under investigation is fully defined in terms of certain parameters that characterize the system, namely the Casson parameter β, the unsteadiness parameter A, the Reynolds number Re, , the magnetic Reynolds number Rm, and the Prandtl number Pr. To simplify the analysis, the governing partial differential equations are transformed into a system of ordinary differential equations using appropriate similarity transformations. The resulting equations are then solved numerically using the collocation method implemented through the MATLAB function bvp4c. This study aims to investigate the effects of the characterizing parameters on the skin friction in the system, Nusselt number, steadiness parameter and free surface temperature are analysed and discussed in detail. Fluid velocity initially decreases with increasing unsteadiness parameter and temperature decreases significantly due to unsteadiness. Increasing the Casson parameter suppresses the velocity field but enhances the temperature. The results show that an increase in magnetic parameter, the velocity boundary layer thickness decreases. The presence of transverse magnetic field sets in the Lorentz force which disturbs the Casson fluid flow hence inducing the retarding on the velocity field. These results indicate the potential technological uses of stretchable materials in liquid-based systems, specifically in applications like paint spray for motor vehicles. Several of our computational findings align with existing data in the literature, although discrepancies arise due to the influence of the induced magnetic field.**

Keywords: **Boundary Layer Theory; Casson Fluid Model; Viscous Casson Fluid, Magneto-hydrodynamics (MHD); Mathematical Modelling; Similarity Transformation; Stretching Sheet.**

I. INTRODUCTION

In recent years, there has been a growing interest in the analysis of non-Newtonian fluids in boundary layer situations due to their wide range of applications in industries such as polymers, paper manufacturing, and food production. While various models have been developed to capture the complex behaviours of non-Newtonian fluids, no single model can fully encompass all their physical characteristics. For example, the Power-Law model can describe both shear-thinning and shear-thickening behaviours but does not account for normal stress differences. On the other hand, the Maxwell model, a basic viscoelastic model, can predict the impact of fluid relaxation time on boundary layer dynamics. The Casson model, which is recognized for its shear-thinning nature and yield stress, is commonly used in modelling human blood due to its unique attributes.

Recently, the examination of electrically conducting Casson fluid flow, particularly in the presence of a magnetic field, has emerged as a critical area in applied mathematics. Researchers have studied various physical parameters, like the magnetic parameter and Casson fluid parameters, and their influence on velocity profiles, heat transfer, temperature, and pressure profiles. However, previous studies have primarily focused on externally applied magnetic fields at different orientations, overlooking the effects of induced magnetic fields on fluid flow and skin friction.

To bridge this research gap, the present study seeks to explore the impacts of induced magnetic fields on Casson fluid flow over a stretching sheet by integrating magnetic induction equations into the governing equations. Specifically, this investigation will analyse the influence of the magnetic Reynolds number (Rm) and Reynolds number (Re) on the induced magnetic field.

Numerous researchers have delved into the topic of Casson fluid flow over a stretching sheet, laying the groundwork for the current research endeavour. For instance, the initial investigation into magneto-hydrodynamic (MHD) flows conducted by Faraday in 1939 utilized mercury flowing through a glass tube positioned between magnetic field poles. Faraday proposed harnessing tidal currents within the Earth's magnetic field for power generation. A subsequent study [1] examined the characteristics of MHD Casson fluid flow, heat transfer, and mass transfer in a parallel plate channel with stretching walls under the influence of a uniform transverse magnetic field. The researchers employed the Runge-Kutta fourth-order shooting method to analyse the system. Their findings indicated that increasing the strength of the magnetic field led to a decrease in fluid velocity but an increase in temperature. Another investigation [2] focused on the unsteady two-dimensional flow of a non-Newtonian fluid over a stretching surface. The researchers employed similarity transformations and the shooting method to solve the transformed equations. They observed that fluid velocity decreased as the unsteadiness parameter increased, and the temperature significantly decreased due to the presence of unsteadiness

Further research conducted by [3] examined the effects of cross diffusion and aligned magnetic fields on Casson fluid flow along a stretched surface with variable thickness. The study revealed that higher magnetic interaction numbers suppressed the velocity field while enhancing the concentration and thermal fields. Additionally, [4] investigated Casson fluid flow over vertical porous surfaces with chemical reactions and the presence of a magnetic field. The researchers employed similarity analysis, the Newton-Raphson shooting method, and the fourth-order Runge-Kutta algorithm. Their findings indicated that increasing the magnetic and Casson parameters resulted in a decrease in velocity.

Other research by [5] analysed MHD stagnation point flow of a Casson fluid over a nonlinearly stretching sheet with viscous dissipation, employing the Keller Box method to solve the coupled non-linear ordinary differential equations. They found that increasing the Casson fluid parameter decreases both fluid velocity and temperature but increases the heat and wall skin-friction coefficient. Additional studies by [6] explored the effects of Lorentz force, viscous dissipation, and internal heating on the heat and flow characteristics of a non-Newtonian Casson fluid thin film resting on a stretching surface under a magnetic field. These studies noted that Lorentz force and the non-Newtonian nature of the fluid have a thinning influence on the film. Investigations by [7] into MHD Casson fluid flow over exponentially stretching sheets with radiation effects have also been conducted. These studies analysed the impact of various parameters, such as the Casson parameter, radiation parameter, magnetic parameter, and heat source/sink, on velocity and temperature profiles using iterative perturbation methods. Similarly, research by [8] on the flow and heat transfer of Casson fluid over permeable vertical stretching surfaces considering magnetic and thermal radiation effects has shown that magnetic parameters reduce flow profiles, and increased wall suction decreases boundary layer thickness and velocity.

Recently, studies by [9] have examined electrically conducting fluid in the presence of a uniform transverse magnetic field at the plate, using explicit finite difference methods to approximate velocity, temperature, and concentration. These studies found that heat generation enhances fluid velocity. Additional research by [10] has focused on the effects of radiation on MHD boundary layer flow of Casson fluid over exponentially stretching sheets, using Casson models to characterize non-Newtonian fluids. They found that surface shear stress increases with magnetic and Casson parameters, while heat transfer rates increase with Prandtl number but decrease with magnetic and radiation parameters.

Other notable studies include analysing heat transfer characteristics of steady two-dimensional MHD shear thickening Casson fluid across vertical stretching sheets with variable heat surfaces, using similarity transformations and numerical methods. These studies found that increased suction/injection parameters decrease velocity and temperature distributions. Research by [11] on entropy generation and Hall current effects on MHD Casson fluid over stretching surfaces with velocity

ISSN 2348-1218 (print)
International Journal of Interdisciplinary Research and Innovations ISSN 2348-1226 (online)
Vol. 12, Issue 2, pp: (55-66), Month: April 2024 - June 2024, Available at: www.researchpublish.com

slip factors revealed that entropy generation is enhanced with magnetic parameters, Reynolds number, and group parameters. The research cited above motivates the current study, which aims to address the effects of induced magnetic fields on an unsteady viscous Casson fluid flow with suction over a stretching sheet. By introducing magnetic induction equations derived from Ohm's law into the governing equations, this study seeks to provide a more comprehensive understanding of the impact of magnetic fields on Casson fluid flow dynamics.

This study will evaluate previous investigations and bring new insights by incorporating magnetic induction equations into the analysis of unsteady incompressible viscous Casson fluid flow. This approach has garnered significant interest among current mathematicians and aims to bridge the existing research gap in understanding the effects of induced magnetic fields on Casson fluid flow and skin friction.

II. MATHEMATICAL FORMULATION

A. Description of The Flow Problem

Consider the unsteady flow of two-dimensional laminar flow of an electrically conducted viscous incompressible Casson fluid over a stretching sheet, we assume that the surface stretching velocity is $U_w = \frac{cx}{(1-\alpha t)}$ as defined by [2], where c is the initial stretching rate of the sheet. Magnetic field is expressed by $B = \frac{B_0}{\sqrt{(1-\alpha t)}}$ and is proposed to be normal to the direction of the stretching sheet with admission of transverse velocity. Furthermore, the sheet is stretched along the $x-axis$ as shown in Fig. 2.1. Meanwhile, the flow is considered under the suction effects at the boundary layer.

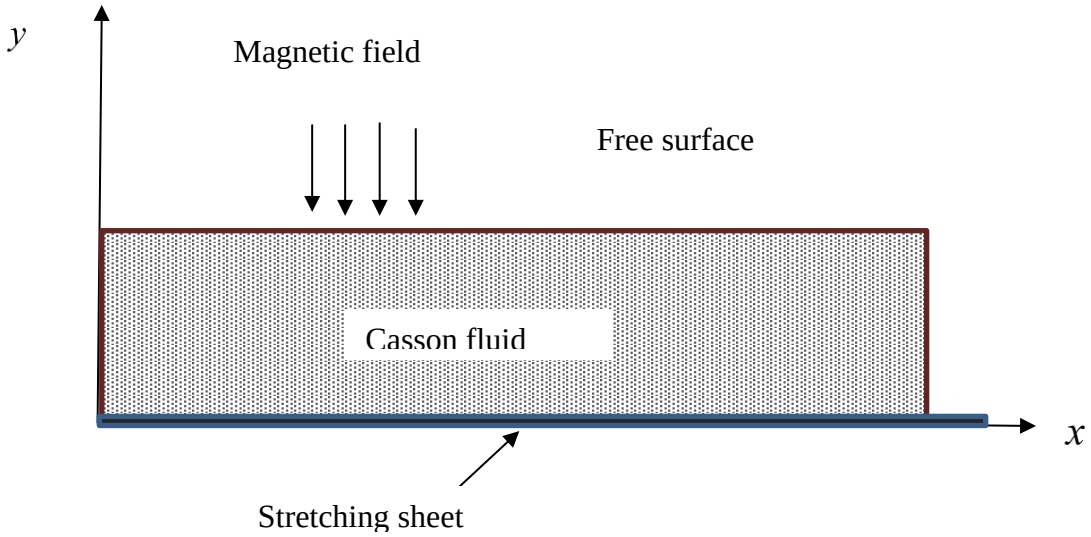

Fig.1: Flow geometry

Furthermore, the presence of an induced magnetic field is taken into consideration, with the external electric field being deemed insignificant as a result of charge polarization within the fluid flow. Additionally, given that the fluid under investigation is electrically conductive and in motion due to the movement of the sheet, an induced magnetic field is present. This induction of a magnetic field results in the generation of Alfven's waves, as illustrated in Fig.2 below. Consequently, the movement of the fluid causes the induced magnetic field (B_0) to be pulled in the direction of the fluid flow. This pulling action gives rise to a force known as the Lorentz force, which opposes the movement of the magnetic field, as depicted in the diagrams in Fig. 2. This process occurs repeatedly, leading to the creation of an induced magnetic field.

ISSN 2348-1218 (print)
International Journal of Interdisciplinary Research and Innovations ISSN 2348-1226 (online)
Vol. 12, Issue 2, pp: (55-66), Month: April 2024 - June 2024, Available at: www.researchpublish.com

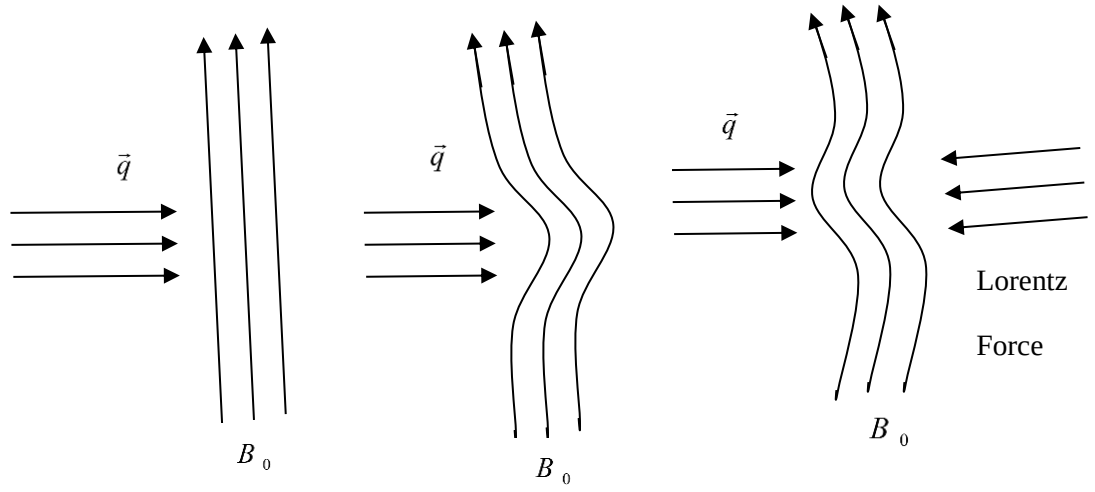

Fig. 2: Formations of Alfve'n waves

B. General Governing Equations

The general equations governing the considered Casson fluid flow are;

$$\frac{\partial \rho}{\partial t} + \vec{\nabla} \cdot (\rho \, \vec{q}) = 0 \tag{1}$$

$$\frac{\partial \vec{q}}{\partial t} + (\vec{q} \cdot \vec{\nabla})\vec{q} - \frac{1}{\rho}\vec{\nabla} p + \nu \nabla^2 \, \vec{q} + \frac{1}{\rho}\vec{F} \tag{2}$$

$$\rho c_p \left(\frac{\partial T}{\partial t} + \vec{q}\vec{\nabla} T \right) = K \nabla^2 T + \mu \Phi \tag{3}$$

$$\frac{\partial \vec{B}}{\partial t} = \vec{\nabla} \times (\vec{q} \times \vec{B}) + \eta_0 \vec{\nabla}^2 \vec{B} \tag{4}$$

To derive the specific equations governing the Casson fluid flow, the following assumptions are considered;

i. The fluid is incompressible and electrically conducting.

ii. There are no externally applied electric fields, $\vec{E} = 0$

iii. The fluid flow is laminar, two dimensional, and initiated by the stretching of the sheet.

iv. The pressure gradient and gravitational force are negligible.

v. The external magnetic field is applied perpendicular to the fluid flow.

By taking into account the aforementioned assumptions in conjunction with the fluid flow description provided in section *A*, we obtain.;

$$\vec{q} = u\hat{i} + v\hat{j} + 0\hat{k}, \quad \vec{B} = b\hat{i} + B_0 \hat{j} + 0\hat{k} \tag{5}$$

From assumption (iv), we write;

$$\vec{\nabla} p = 0 \tag{6}$$

ISSN 2348-1218 (print)
International Journal of Interdisciplinary Research and Innovations ISSN 2348-1226 (online)
Vol. 12, Issue 2, pp: (55-66), Month: April 2024 - June 2024, Available at: www.researchpublish.com

In a Casson fluid flow, the viscosity coefficient is expressed dynamically as follows by considering the rheological equation describing flow matter of the Casson fluid as defined by [12].

$$\tau_{ij} = \begin{cases} 2\left(\mu_B + p_y \big/ \sqrt{2\pi_c}\right)e_{ij}, \pi \lhd \pi_c \\ 2\left(\mu_B + p_y \big/ \sqrt{2\pi}\right)e_{ij}, \pi \rhd \pi_c \end{cases}$$

Where;

$e_{ij} = \frac{1}{2}\left(\frac{\partial u_i}{\partial x_j} + \frac{\partial u_j}{\partial x_i}\right)$ is the rate of strain tensor; u_i are the velocity components.

p_y is the yield stress of the Casson fluid expressed as,

$$p_y = \frac{\mu_\beta \sqrt{2\pi}}{\beta}$$

From the definition of viscosity given by Isaac Newton, the ratio of shear stress τ^* to viscosity μ is constant for a Newtonian case.

$$\tau^* = \mu \frac{\partial u}{\partial y}$$

Some fluids require a gradually increasing shear stress to maintain a constant strain rate and are called Rheopectic, in the case of Casson fluid (non-Newtonian) flow where $\pi \rhd \pi_c$, therefore,

$\mu = \mu_\beta + \frac{p_y}{\sqrt{2\pi}}$ Hence, the kinematic viscosity can be written as;

$$\nu = \frac{\mu_\beta}{\rho}\left(1 + \frac{1}{\beta}\right)$$

τ_{ij} is the $(i, j) - th$ component of the stress tensor, $\pi = e_{ij}e_{ij}$ and e_{ij} are the $(i, j) - th$ component of the deformation rate, π is the product of deformation rate with itself, π_c is a critical value of this product based on the non-Newtonian model, μ_B is the plastic dynamic viscosity of the non-Newtonian Casson fluid, where β is the Casson parameter. If a shear stress less than yield stress is applied to the fluid, it behaves like a solid, whereas if a shear stress greater than yield stress is applied, the fluid flows and deformation starts.

Henceforth, by using the vector expressions stated in equation (5), the specific governing equations resulting from the aforementioned physical assumption of Casson fluid flow are presented below.

C. Specific Governing Equations

These specific governing equations are derived from the general equations

$$\frac{\partial u}{\partial x} + \frac{\partial v}{\partial y} = 0 \qquad (7)$$

ISSN 2348-1218 (print)
International Journal of Interdisciplinary Research and Innovations ISSN 2348-1226 (online)
Vol. 12, Issue 2, pp: (55-66), Month: April 2024 - June 2024, Available at: www.researchpublish.com

$$\frac{\partial u}{\partial t}+u\frac{\partial u}{\partial x}+v\frac{\partial u}{\partial y}=\upsilon\left(1+\frac{1}{\beta}\right)\frac{\partial^2 u}{\partial y^2}+\frac{\sigma}{\rho}\left(B_0 vb-uB_0{}^2\right) \quad (8)$$

$$\frac{\partial T}{\partial t}+u\frac{\partial T}{\partial x}+v\frac{\partial T}{\partial x}=K\frac{\partial^2 T}{\partial y^2}+\frac{Q_0}{\rho c_p}\left(T-T_\infty\right) \quad (9)$$

$$\frac{\partial}{\partial y}\left(uB_0-vb\right)+\eta_0\frac{\partial^2 b}{\partial y^2}=0 \quad (10)$$

Since $b=b(y)$ and B_0 is a constant.

The boundary conditions accompanying the above specific governing equations are;

At $u=U_w(x,t),\quad v=0,\quad T=T_w(x,t),\quad b=B_0\ at\ y=o$

As $u\to 0,\quad T\to\infty,\quad b\to 0,\ as\ y\to\infty$

III. METHOD OF SOLUTIONS

A. Transformation of Equations and Boundary Conditions through Similarity Techniques

The equations provided in section ***C*** are subject to a similarity transformation above to ordinary differential equations becomes;

$$\eta=\sqrt{\frac{c}{\upsilon(1-\alpha t)}}y,\quad \psi=\sqrt{\frac{\upsilon c}{1-\alpha t}}xf(\eta),$$

$$b=\frac{cx}{1-\alpha t}g'(\eta),\quad T=T_\infty+\left[\frac{T_0 cx^2(1-\alpha t)^{-\frac{3}{2}}}{2\upsilon}\right]\theta(\eta)$$

Where, η is the dimensionless similarity variable, ψ is the stream function defined as;

$$u=\frac{\partial\psi}{\partial y},\quad v=-\frac{\partial\psi}{\partial x}$$

Applying the aforementioned transformations to the boundary conditions outlined in section C yields the following result:

- When $y=0$, we obtain

$$\eta=0;\quad f'=1;\quad f(0)=0;\quad \theta=1$$

- When $y\to\infty$; we get;

$$\eta\to\infty;\quad f'(\infty)=0;\quad \theta(\infty)=0;\quad g'(\infty)=0$$

The transformed specific governing ordinary differential equations are given below;

$$\left(1+\frac{1}{\beta}\right)f'''+ff''-f'^2-M\left(\sqrt{\frac{\upsilon c}{1-\alpha t}}B_0{}^{-1}fg'-f'\right)-A\left(f'+\frac{\eta}{2}f''\right)=0 \quad (11)$$

ISSN 2348-1218 (print)
International Journal of Interdisciplinary Research and Innovations ISSN 2348-1226 (online)
Vol. 12, Issue 2, pp: (55-66), Month: April 2024 - June 2024, Available at: www.researchpublish.com

$$\Pr^{-1}\theta''+f\theta'-2f'\theta+\lambda\theta-\frac{A}{2}(\eta\theta'+3\theta)=0 \quad (12)$$

$$g'''-\frac{R_m}{R_e}fg''-\frac{R_m}{R_e}f'g'-B_0\frac{R_m}{R_e}\sqrt{\frac{1-\alpha t}{c\upsilon}}f''=0 \quad (13)$$

Meanwhile, the physical parameters associated with the aforementioned transformed governing equations are also specified as outlined below.

Magnetic parameter; $M=\frac{\sigma B_0^2}{c\rho}(1-\alpha t)$

Skin friction coefficient; $Cf_x=\frac{\tau_w}{\rho u^2}$

Nusselt number; $Nu_x=\frac{xq_w}{\kappa(T-T_\infty)}$

Magnetic Reynolds number; $R_m=\mu_0\sigma UL_0$

Prandtl parameter number; $\Pr=\frac{\upsilon}{\alpha}=\frac{c_P\mu}{K}$

Reynolds number; $\mathrm{Re}=\frac{\rho UL}{\mu}=\frac{UL}{\upsilon}$

B. Numerical Methods of Solution

The three specific ordinary differential equations (11), (12) and (13) obtained in section ***A*** are reduced from higher order into a first order as follows;

Equation (11), is reduced by letting;

$$z_1=f,\ z_2=f',\ z_3=f'',\ z_4=g,\ z_5=g',\ z_6=g''$$

Which yields the following system of differential equations;

$$z'_1=z_2$$

$$z'_2=z_3$$

$$z'_3=\frac{1}{(1+\beta^{-1})}\left(-z_1z_3+z_2^2+M\left(\sqrt{\frac{\upsilon c}{1-\alpha t}}B_0z_1z_5-z_2\right)+A\left(z_2+\frac{\eta}{2}z_3\right)\right) \quad (14)$$

Further, equation (12) is reduced by letting,

$$z_7=\theta,\ z_8=\theta'$$

Which yields the following system of differential equations

$$z'_7=z_8$$

ISSN 2348-1218 (print)
International Journal of Interdisciplinary Research and Innovations ISSN 2348-1226 (online)
Vol. 12, Issue 2, pp: (55-66), Month: April 2024 - June 2024, Available at: www.researchpublish.com

$$z'_8 = pr\left(-z_1 z_8 + 2z_2 z_7 - \lambda z_7 + \frac{A}{2}(\eta z_8 + 3z_7)\right) \quad (15)$$

Moreover, equation (13) is also reduced to a first order ordinary differential equation by letting;

$$z'_4 = z_5$$
$$z'_5 = z_6$$

$$z'_6 = \frac{R_m}{R_e}\left(-z_1 z_6 - z_2 z_5 - B_0\sqrt{\frac{1-\alpha t}{c\upsilon}}z_3\right) \quad (16)$$

IV. RESULTS AND DISCUSSIONS

A. The impact of induced magnetic induction on skin friction and Nusselt number.

Utilizing a collocation technique for solving the aforementioned first order systems of ordinary differential equations via the MATLAB function bvp4c, we establish the correlation among skin friction, Nusselt Number, and various dimensionless parameters employed in this investigation, as illustrated in Table 1.

TABLE I: SKIN FRICTION NUSSELT NUMBER IN RELATION TO DIFFERENT DIMENSIONLESS PARAMETER

β	C_f	Nu_x
A =4, λ =-1		
0.1	-6.1354	2.6006
0.2	-4.5743	2.5888
0.3	-3.9159	2.5812
A =4, λ =1		
0.1	-6.1354	2.2816
0.2	-4.5743	2.2665
0.4	-3.5397	2.2497
A =1, λ =-1		
0.1	-3.4552	1.9881
0.2	-2.5534	1,9749
0.4	-1.9807	1.9589
A =1, λ =1		
0.1	-3.4552	1.5250
0.2	-2.5534	1.5001
0.4	-1.9807	1.4689

The variation of the local skin friction coefficient and Nusselt number for different values of unsteadiness parameter A and Casson parameter β are depicted in table 1. It can be easily seen that an increase of the Casson parameter β leads to increase the local skin friction coefficient C_f and decrease the local Nusselt number.

B. The Impact of Physical Parameters on Fluid Flow Patterns in the Presence of an Induced Magnetic Field.

The graphical representation, analysis, and discussion of the results obtained from altering the physical characteristic parameters are presented.

ISSN 2348-1218 (print)
International Journal of Interdisciplinary Research and Innovations ISSN 2348-1226 (online)
Vol. 12, Issue 2, pp: (55-66), Month: April 2024 - June 2024, Available at: www.researchpublish.com

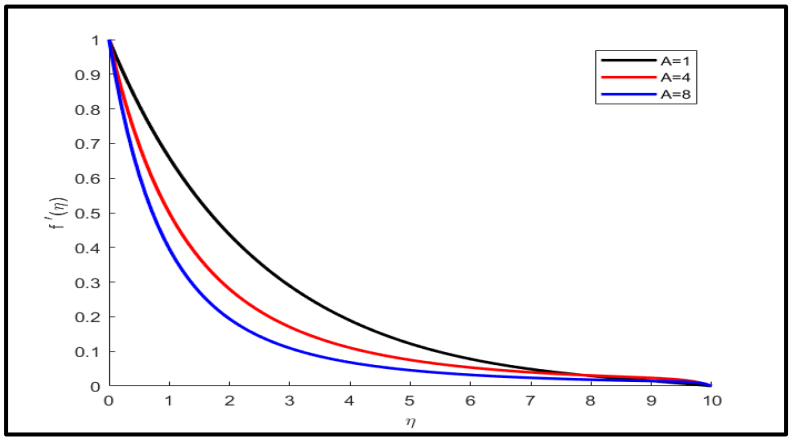

Fig. 3: Fluid velocity for different values of A

Fig.3, exhibits the velocity profile for several values of unsteadiness parameter A. it is seen that the velocity along the sheet decreases initially with the increase in unsteadiness parameter A, and this implies an accompanying reduction of the momentum boundary layer thickness near the wall.

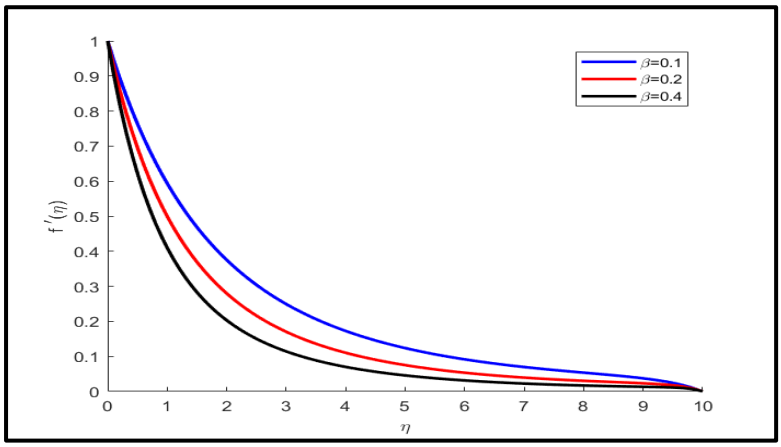

Fig. 4: Fluid velocity for different values of β

Fig. 4, presents the velocity profile corresponding to different values of Casson fluid parameter β . It highlights the slowed stream flow of the stretching sheet as β is enhanced. This is due to the drop in yield stress at higher values of β which causes the fluid to behave more like Newtonian fluid, hence the velocity is seen to decrease. We also note that Casson parameter makes the velocity boundary layer thickness shorter. This occurs because of the plasticity of Casson fluid.

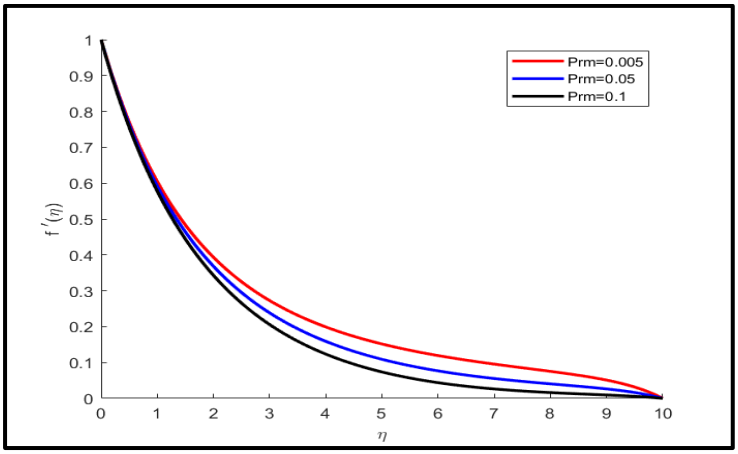

Fig. 5: Velocity profile for different values of prm

ISSN 2348-1218 (print)
International Journal of Interdisciplinary Research and Innovations ISSN 2348-1226 (online)
Vol. 12, Issue 2, pp: (55-66), Month: April 2024 - June 2024, Available at: www.researchpublish.com

Fig.5, depicts the velocity graph in relation to the magnetic parameter prm illustrates the discrepancy. As the magnetic parameter prm increases, the thickness of the velocity boundary layer diminishes. The introduction of a transverse magnetic field generates the Lorentz force, which acts against the flow of the Casson fluid, thereby exerting a retarding force on the velocity field. Consequently, as the magnetic parameter values increase, the retarding force intensifies, leading to a decrease in both the velocity and the thickness of the velocity boundary layer.

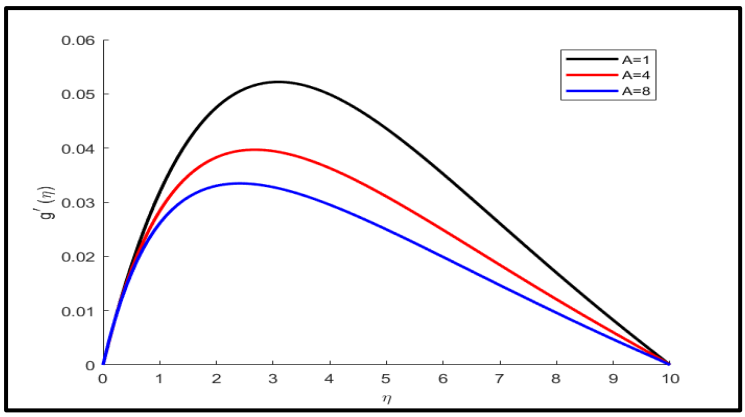

Fig.6: Magnetic induction profile for various values of A

From Fig. 6, the magnetic induction diminishes as the unsteadiness parameter A rises. An increase in the unsteadiness parameter leads to a decrease in fluid velocity caused by the thickening of the boundary layer and the impact of viscous drag, ultimately causing a reduction in magnetic induction.

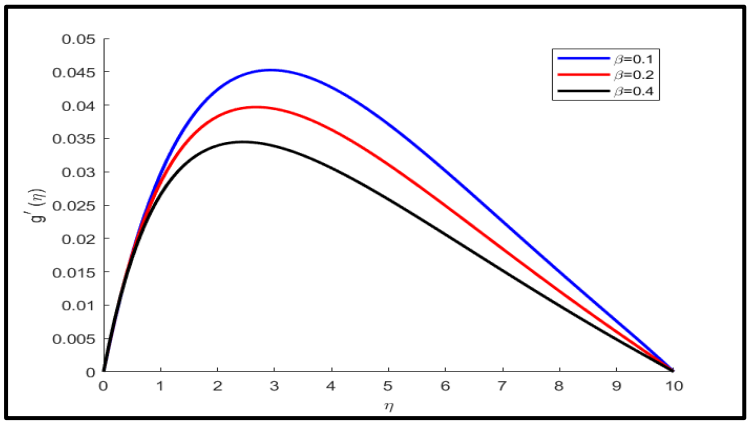

Fig. 7: Magnetic induction profile for different values of β

In Fig. 7, it is noticed that, an increase in Casson parameter β reduces the magnetic induction profile.

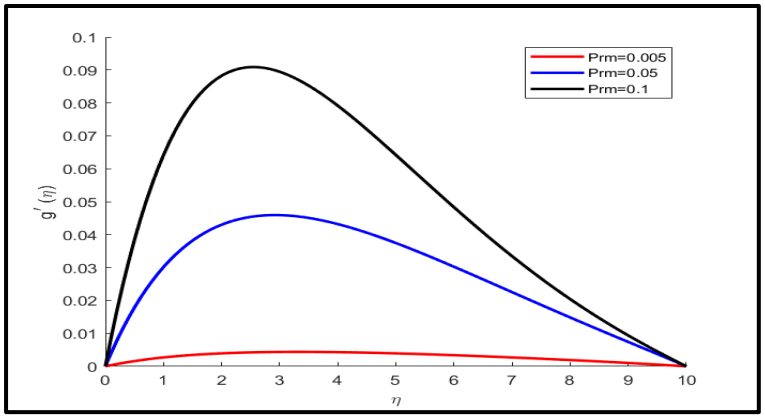

Fig. 8: Magnetic induction profile for different values of prm

ISSN 2348-1218 (print)
International Journal of Interdisciplinary Research and Innovations ISSN 2348-1226 (online)
Vol. 12, Issue 2, pp: (55-66), Month: April 2024 - June 2024, Available at: www.researchpublish.com

Fig. 8, shows that, the magnetic induction rises as the magnetic parameter prm increases. The augmentation of the magnetic parameter prm results in a reduction of viscous forces, thereby causing an escalation in the velocities of fluid molecules and ultimately leading to an amplified magnetic induction.

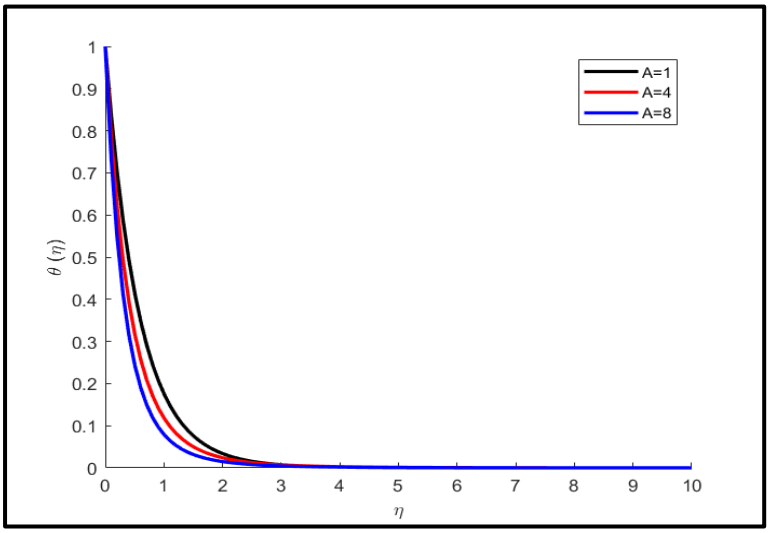

Fig. 9: Temperature profile of different values of A

Fig. 9, the results indicate a notable decrease in temperature profiles as the unsteadiness parameter rises. As the value of the unsteadiness parameter A increases, the heat transfer rate from the sheet to the fluid diminishes. Consequently, less heat is transferred from the sheet to the fluid with an increase in the unsteadiness parameter. This leads to a decrease in the temperature profile $\theta(\eta)$. Due to the fact that the fluid flow is induced by the stretching sheet and the sheet surface temperature exceeds the free stream temperature, both the fluid velocity and temperature decrease as the unsteadiness parameter A increases. From the above observation, it is important to note that, the rate of cooling is much faster for higher values of unsteadiness parameter.

V. CONCLUSIONS

The present study provides the numerical solutions for the unsteady magnetic induction effects on Casson fluid flow over a stretching sheet. The effect of various fluid flow physical parameters on Casson fluid velocity, Numerical investigations have been conducted to examine the effects of induced magnetic field and skin friction. The governing nonlinear partial differential equations (PDEs) derived from the momentum, temperature, and induction equations are converted into a system of ordinary differential equations (ODEs) through the application of similarity transformations. These equations are then solved using bvp4c MATLAB solver. From the study, the following conclusions have been drawn during this investigation.

1. Fluid velocity initially decreases with increasing unsteadiness parameter and temperature decreases significantly due to unsteadiness.
2. Velocity profile decreases with increasing Casson parameter but temperature in this case increases.
3. Increase of magnetic field parameter decreases the velocity boundary layer thickness.
4. Thermal boundary layer thickness decreases with the increasing Prandtl number, so it can be used to increase the rate of cooling in conducting fluid.
5. The magnitude of heat transfer rate at the surface decreases for Casson parameter β and unsteadiness parameter A.
6. Skin friction decreases with increasing unsteadiness parameter A.
7. The magnetic induction decreases as the unsteadiness parameter A increases.
8. The magnetic parameter retards the velocity of the flow field due to the magnetic pull of the Lorentz force acting on the flow field.

REFERENCES

[1] Sarojamma, G. (2014). *MHD Casson Fluid Flow , Heat and Mass Transfer in a Vertical Channel with Stretching Walls*. *2*(10), 800–810.

[2] Mukhopadhyay, S., De, P. R., Bhattacharyya, K., & Layek, G. C. (2013). Casson fluid flow over an unsteady stretching surface. *AIN SHAMS ENGINEERING JOURNAL*. https://doi.org/10.1016/j.asej.2013.04.004.

[3] Saravana,R., Sailaja,M, and Hemadri Reddy, R. (2018). Effect of Aligned Magnetic Field on Casson Fluid Flow over a Stretched Surface of Non-uniform thickness, htt:doi.org/10.1515/nleng-2017-0173.

[4] Arthur, E. M., Seini, I. Y., & Bortteir, L. B. (2015). Analysis of Casson Fluid Flow over a Vertical Porous Surface with Chemical Reaction in the Presence of Magnetic Field. *June*, 713–723.

[5] Medikare, M., Joga, S., & Chidem, K. K. (2016). MHD Stagnation Point Flow of a Casson Fluid over a Nonlinearly Stretching Sheet with Viscous Dissipation. *March*, 37–48.

[6] Vijaya, N., Sreelakshmi, K., & Sarojamma, G. (2016). Effect of Magnetic Field on the Flow and Heat Transfer in a Casson Thin Film on an Unsteady Stretching Surface in the Presence of Viscous and Internal Heating. 303–320. https://doi.org/10.4236/ojfd.2016.64023

[7] Mohammed, I.B.S, Saidu Yakubu.Vulegbo and Mohammed Issa. (2019). Magnetohydrodynamic Casson Fluid Flow over an Exponential Stretching Sheet with Effect of Radiation, African scholar publicationa and research international, Vol.15. no.9,Pp.172-180.

[8] Hasan M M and Zillur Raman. (2019). Casson Fluid Flow and Heat Transfer over a Permeable Vertical Stretching Surface with Magnetic Field and Thermal Radiation, IOSR Journal of Engineering (IOSORJEN) Vol. 09,no.01,2019,Pp.14-19.

[9] Omokhuale,E., Jabika,M.L. (2019). Magnetohydrodynamic Casson Fluid over an Vertical Plate with Chemical Reaction and Heat Generation, American Journal of computational Mathematics, Vol.09.03(2019),Article ID:95414, 14 pages 10.4236/ajcm.2019.93014.

[10] Ishfaq Ahmad Tantry, Shamasuddin Wani and Dr. Bhawna Agrawal.(2020). Study of MHD Boundary Layer Flow of a Casson Fluid due to an Exponentially Stretching Sheet with Radiation Effect, International jounal of statiatics and Applied Mathematics 2020; 6(1):138-144.

[11] Ramudu, A. C. V., Kumar, K. A., & Sandeep, V. S. N. (2020). Influence of suction / injection on MHD Casson fluid flow over a vertical stretching surface. *7*, 3675–3682.

[12] Rehman, S., Idrees, M., Shah, R. A., & Khan, Z. (2019). Suction / injection effects on an unsteady MHD Casson thin film flow with slip and uniform thickness over a stretching sheet along variable flow properties. *Bound Value Probl*, *0*, 1–25. https://doi.org/10.1186/s13661-019-1133-0